Supporting Information for:

Promoted solubilization and desorption of petroleum hydrocarbons to remediate contaminated soils using Pickering emulsions stabilized by cellulose nanocrystals

Yi Yang [a], Yi Ma [a], Tingting Huang [a], Xiaoming Song [b], Yinqing Zhang [a, *], Lingyan Zhu [a]

[a] Key Laboratory of Pollution Processes and Environmental Criteria, Ministry of Education, Tianjin Key Laboratory of Environmental Remediation and Pollution Control, College of Environmental Science and Engineering, Nankai University, Tianjin 300350, China

[b] Key Laboratory of Eco-restoration of Regional Contaminated Environment, Ministry of Education, Shenyang University, Shenyang 110044, China

*To whom correspondence should be addressed.

E-mail address: yinqing.zhang@nankai.edu.cn

Phone: +86-22-23500791

Isolation of cellulose

The isolation of cellulose was composed of pre-treatment and delignification steps following the previous studies with some modifications.[1, 2] Rice straw was first soaked in hot water to remove dirt and aqueous soluble substances. For bleaching, the dried rice straw powder (30 g) was subjected to 450 mL toluene/ethanol (2:1, v/v) mixture for 20 h, followed by oven-drying at 55 °C for 24 h. The powder was then immersed in 1.4 wt% acidified $NaClO_2$, with pH adjusted to 3-4 by CH_3COOH, at 70 °C for 5 h to dissolve lignin. After quenching the reaction with ice and decanting the excess liquid, the light-yellow solid was washed with deionized water until the filtrate became neutral pH. Hemicellulose and silica in the delignified powder were leached with 600 mL 5% KOH at room temperature for 24 h and then at 90 °C for 2 h. The obtained white cellulose powder was centrifuged and washed with deionized water until the filtrate became neutral pH. Afterwards, the mixture was freeze-dried and denoted as raw celluloses (RCs).

Quantification of sulfate and formyl groups contents

The sulfate groups and formyl groups contents were determined using an automatic potentiometric titration instrument. The freeze dried CNCs (0.1 g) was dissolved in 2 mL 0.1 M NaOH solution, and the suspension was stirred at 60 °C for 8 h to dissociate sulfate and formyl groups from CNCs. The mixture was then diluted to 20 mL with deionized water, and further acidified with 2.5 mL 0.1 M HCl solution. Then, 0.5 mL 0.001 M NaCl solution was added, and the final mixture was titrated with pre-calibrated 0.01 M NaOH solution automatically. At the beginning stage of the titration curves, the conductivity decreased linearly with the addition of NaOH standard solution until the first equivalence point appeared due to the consumption by protons associated with the H_2SO_4 and excessive HCl. Then, the conductivity changed slowly with an apparent platform and the protons associated with the dissociation of formyl groups were neutralized during this period. Based on the consumption of NaOH at the two equivalence points, the contents of sulfate and formyl group can be calculated according to the following empirical equations, respectively.

$$c_{sulfate} \ (\text{mmol·g}^{-1}) = (0.2 + c_2 V_2 - c_1 V_1)/m$$

$$c_{formyl} \ (\text{mmol·g}^{-1}) = c_2(V_3 - V_2)/m$$

where $c_{sulfate}$ and c_{formyl} (mmol·g^{-1}) represent the contents of sulfate and formyl groups, respectively; c_1 and c_2 (M) represent the concentration of HCl standard solution and NaOH standard, respectively; V_1 (mL) is the consumed volume of HCl standard solution; V_1 and V_2 (mL) are the consumed volume of NaOH standard solution at the first and second equivalence point, respectively; m (g) represent the weight of CNCs.

Preparation of contaminated soil

The pre-contaminated soil was prepared according to the previous procedures with slight modifications.[3-5] The experimental soil was collected from an uncontaminated top soil in Hebei Province, China and screened through a 2-mm sieve to remove large coarse materials such as leaves and stones. Tetradecane-contaminated soil was prepared by mixing 50 mL acetone containing 5 g tetradecane with per kilogram soil. The mixtures were stirred in the fume hood until the acetone evaporated off and the moisture content was less than 1% as determined by oven drying of soil at 105 °C for 24 h.[6] The artificially contaminated soil was aged for three months under dark and ventilated conditions.

Quantification of tetradecane

For the solid phase, an aliquot of 0.5 g homogenized and frozen-dried soil was mixed with 10 mL dichloromethane in a glass centrifugal tube. The mixture was shaken at 250 rpm for 5 h and the supernatant was separated by centrifugation at 10,000 rpm for 15 min. The filtrate was dried under gentle nitrogen flow and reconstituted in 1 mL dichloromethane. After passing through a 0.22 μm nylon membrane, tetradecane was quantified by gas chromatography (GC).

For the liquid phase, the supernatant (5 mL) was mixed with 10 mL dichloromethane and the mixture was shaken at 250 rpm for 5 h. The filtrate was dried under gentle nitrogen flow and reconstituted in 1 mL dichloromethane. After passing through a 0.22 μm nylon membrane, tetradecane was quantified by gas chromatograph (GC, 7890A, Agilent, USA) equipped with a capillary column (DB-5MS-123-5533, 0.32 mm × 30 mm × 1.00 μm).

Detailed information for the GC instrumental analysis is provided below. The inlet temperature was set to 300°C. The column temperature was maintained at an initial temperature of 50°C for 2 min, ramped up to 230°C at a rate of 40°C per minute, then ramped up to 320°C at a rate of 20°C per minute and finally maintained for 20 min. During the procedure, the gas flow rates were maintained high purity nitrogen at 1.5 mL·min^{-1}, hydrogen at 30 mL·min^{-1} and air at 300 mL·min^{-1}. The detector temperature was 325°C with an injection volume of 1.0 μL.

Removal rate calculation

In order to quantitatively compare the removal rate constant k (h^{-1}), the removal kinetics were further estimated by pseudo-first-order law: $\ln (c_t/c_0) = -k \cdot t$, where c_0 and c_t represent the concentrations of tetradecane initially and at the time point t (h), respectively.

Laser particle size measurement

To measure the Pickering emulsion oil droplet diameter, a laser particle size analyzer (Mastersizer 2000G, Malvern, UK) was used with a 633 nm Helium neon laser. The average droplet diameter was calculated from the three replicate measurements of the volume mean diameter ($D_{4/3}$) based on the Mie scattering measurement principle, which could mathematically defined as:

$$D_{4/3} = \frac{\sum D_i^4 N_i}{\sum D_i^3 N_i}$$

Where D_i is the droplet diameter of droplet fraction I and N_i is the droplets number of size D_i. The refractive index of the oil phase used in the Malvern Mastersizer software during measurements.

Two-dimensional correlation spectroscopy (2D-CoS) analysis

To obtain the structural variation information on the FSCNCs-soil interaction, 2D-CoS was employed using FTIR spectra with time as the external perturbation. The 2D-CoS spectra were produced according to the method of Noda and Ozaki.[7] The involved algorithm adopted in the software is given below.

For the perturbation-induced spectral variation $Y(\lambda_i, C_k)$ as a function of a spectral variable (λ, the spectral wavelength of ATR-FTIR) and a perturbation variable (C, desorption time), a set of dynamic spectra $\bar{Y}(\lambda_i, C_k)$ is defined as follows:

$$\bar{Y}(\lambda_i, C_k) = \begin{cases} Y(\lambda_i, C_k) - \bar{Y}(\lambda_i), & 1 \le k \le m \\ 0, & otherwise \end{cases}$$

where $\bar{Y}(\lambda_i)$ denotes the reference spectrum, typically, the m variable-averaged spectrum.

$$\bar{Y}(\lambda_i) = \frac{1}{m} \sum_{k=1}^{m} Y(\lambda_i, C_k)$$

The synchronous (Φ) and asynchronous (Ψ) correlation spectra can be generated from the following transform:

$$\Phi(\lambda_1, \lambda_2) = \frac{1}{m-1} \sum_{k=1}^{m} \bar{Y}(\lambda_1, C_k) \bar{Y}(\lambda_2, C_k)$$

$$\Psi(\lambda_1, \lambda_2) = \frac{1}{m-1} \sum_{k=1}^{m} \bar{Y}(\lambda_1, C_k) \sum_{k=1}^{m} N_{ik} \bar{Y}(\lambda_2, C_k)$$

where the term Nik is the Hilbert-Noda transformation matrix defined as follows:

$$N_{ik} = \begin{cases} 0, & i = k \\ \dfrac{1}{\Pi(k-i)}, & otherwise \end{cases}$$

Synchronous correlation spectrum $\Phi(\lambda_1, \lambda_2)$ corresponding to the real part of the cross-correlation function represent the directionality of two spectral intensities measured at λ_1 and λ_2. If the sign of the cross-peaks $\Phi(\lambda_1, \lambda_2)$ is positive, the spectral

intensities at λ_1 and λ_2 are either increasing or decreasing simultaneously. In reverse, if the direction is opposite, the sign of $\Phi(\lambda_1, \lambda_2)$ becomes negative.

Asynchronous correlation spectrum $\Psi(\lambda_1, \lambda_2)$ reflects that the sequential order of intensity changes of two spectral intensities measured at λ_1 and λ_2 induced by the perturbation.

If the signs of $\Phi(\lambda_1, \lambda_2)$ and $\Psi(\lambda_1, \lambda_2)$ are same, variation in the spectral intensity at λ_1 always occurs prior to that at λ_2. The sequential order is reversed if $\Phi(\lambda_1, \lambda_2)$ and $\Psi(\lambda_1, \lambda_2)$ have the opposite signs. The variations at λ_1 and λ_2 are completely synchronized if $\Psi(\lambda_1, \lambda_2)$ is zero. If $\Phi(\lambda_1, \lambda_2) = 0$, the sequential order of intensity variations becomes indeterminate.

Table S1. 2D-IR-CoS results of the assignments and signs of cross-peaks in synchronous and asynchronous maps of FSCNCs.

Wavenumber (cm^{-1})	Possible assignments	Ref.	Sign[a]		
			750	1033	1716
750	formation of Si–O, Mn–O, or Fe–O	8	+	(+, +)	(+, -)
1033	C–O–C or C–O groups	9		+	(+, -)
1716	C=O group	9			+

[a]: Signs were obtained in the upper-left corner of the maps: +, positive; −, negative
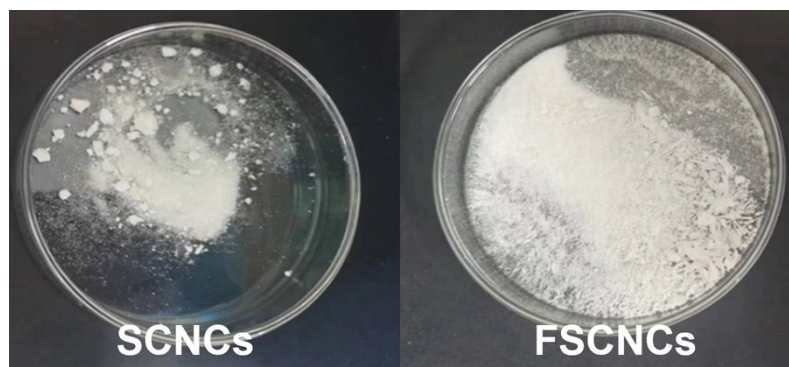
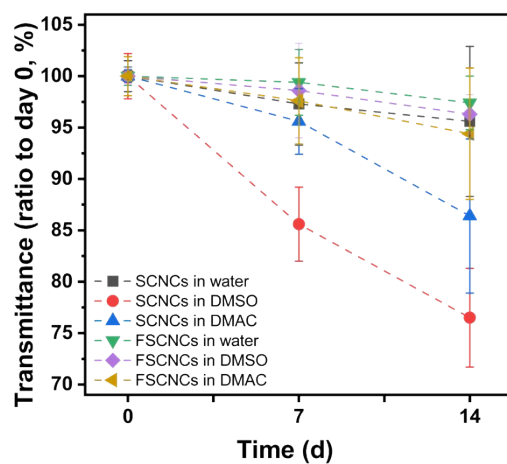**Fig. S1.** Photos of SCNCs and FSCNCs powders.

Fig. S2. Transparency (ratio to day 0, %) of supernatant of CNCs samples in water, DMSO, and DMAC as a function of time.
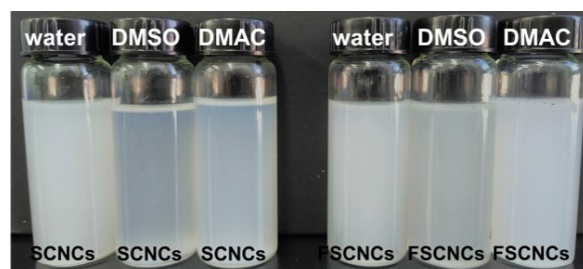
Fig. S3. Dispersibility of SCNCs and FSCNCs in water, DMSO and DMAC, respectively, for more than one month.
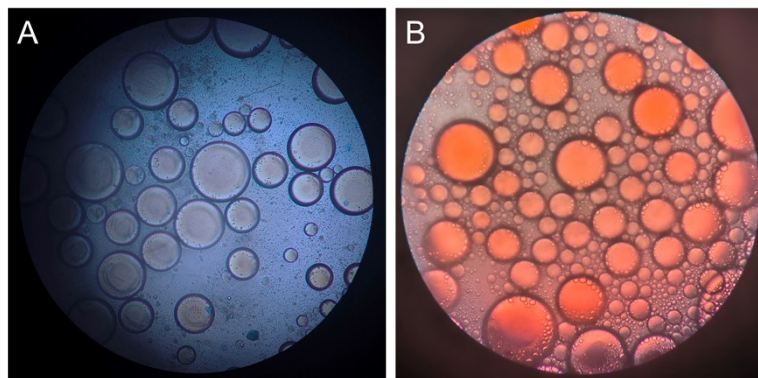
Fig. S4. Optical micrographs of Pickering emulsions stabilized by FSCNCs. (A) Nile blue was added to stain aqueous phase. (B) Nile red and Nile blue were added to stain the oil droplets and aqueous phase, respectively.
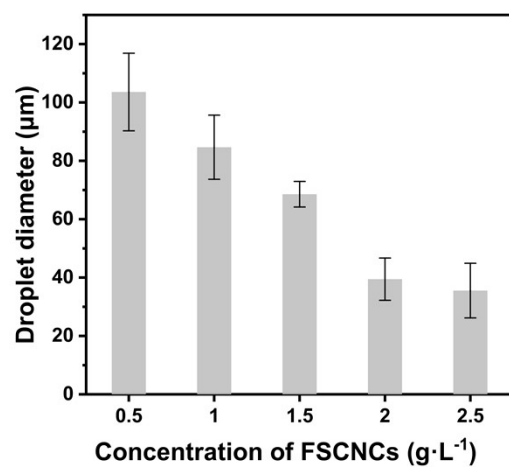
Fig. S5. Average emulsion droplet diameters determined by laser particle size analyzer.

Referneces

1.   P. Lu and Y.-L. Hsieh, Preparation and characterization of cellulose nanocrystals from rice straw, *Carbohydr. Polym.*, 2012, **87**, 564-573.

2.   M. Thakur, A. Sharma, V. Ahlawat, M. Bhattacharya and S. Goswami, Process optimization for the production of cellulose nanocrystals from rice straw derived α-cellulose, *Mater. Sci. Energy Technol.*, 2020, **3**, 328-334.

3.   J. Liu, L. Xu, F. Zhu and S. Jia, Effects of surfactants on the remediation of petroleum contaminated soil and surface hydrophobicity of petroleum hydrocarbon degrading flora, *Environ. Eng. Res.*, 2021, **26**, 200384-200380.

4.   I. Bouzid, J. Maire, S. I. Ahmed and N. Fatin-Rouge, Enhanced remedial reagents delivery in unsaturated anisotropic soils using surfactant foam, *Chemosphere*, 2018, **210**, 977-986.

5.   L. Lu and L. Zhu, Effect of a cationic surfactant on the volatilization of PAHs from soil, *Environ. Sci. Pollut. R.*, 2012, **19**, 1515-1523.

6.   Z. Gong, B. M. Wilke, K. Alef and P. Li, Influence of soil moisture on sunflower oil extraction of polycyclic aromatic hydrocarbons from a manufactured gas plant soil, *Sci. Total Environ.*, 2005, **343**, 51-59.

7.   I. Noda, Close-up view on the inner workings of two-dimensional correlation spectroscopy, *Vib. Spectrosc*, 2012, **60**, 146-153.

8.   X. Yu, W. Liao, Q. Wu, Z. Wei, X. Lin, R. Qiu and Y. Chen, Green remediation of cadmium-contaminated soil by cellulose nanocrystals, *J. Hazard. Mater.*, 2023, **443**, 130312.

9.   H. Wang, H. Du, K. Liu, H. Liu, T. Xu, S. Zhang, X. Chen, R. Zhang, H. Li, H. Xie, X. Zhang and C. Si, Sustainable preparation of bifunctional cellulose nanocrystals via mixed H2SO4/formic acid hydrolysis, *Carbohydr. Polym.*, 2021, **266**, 118107.